Retinopathy Is Reduced during Experimental Diabetes in a Mouse Model of Outer Retinal Degeneration

Tanyth E. de Gooyer,[1] *Kathryn A. Stevenson,*[1] *Pete Humphries,*[2] *David A. C. Simpson,*[1] *Tom A. Gardiner,*[1] *and Alan W. Stitt*[1]

Purpose. Diabetic patients who also have retinitis pigmentosa (RP) appear to have fewer and less severe retinal microvascular lesions. Diabetic retinopathy may be linked to increased inner retinal hypoxia, with the possibility that this is exacerbated by oxygen usage during the dark-adaptation response. Therefore, patients with RP with depleted rod photoreceptors may encounter proportionately less retinal hypoxia, and, when diabetes is also present, there may be fewer retinopathic lesions. This hypothesis was tested in rhodopsin knockout mice ($Rho^{-/-}$) as an RP model in which the diabetic milieu is superimposed. The study was designed to investigate whether degeneration of the outer retina has any impact on hypoxia, to examine diabetes-related retinal gene expression responses, and to assess lesions of diabetic retinopathy.

Methods. Streptozotocin-induced diabetes was created in male C57Bl6 (wild-type; WT) and $Rho^{-/-}$ mice, and hyperglycemia was maintained for 5 months. The extent of diabetes was confirmed by measurement of glycated hemoglobin (%GHb) and accumulation of advanced glycation end products (AGEs). Retinal hypoxia was assessed using the bioreductive drug pimonidazole. The retinal microvasculature was studied in retinal flatmounts stained by the ADPase reaction, and the outer retina was evaluated histologically in paraffin-embedded sections. Retinal gene expression of VEGF-A, TNF-α, and mRNAs encoding basement membrane component proteins were quantified by real-time RT-PCR.

Results. The percentage GHb increased significantly in the presence of diabetes ($P < 0.001$) and was not different between WT or $Rho^{-/-}$ mice. Hypoxia increased in the retina of WT diabetic animals when compared with controls ($P < 0.001$) but this diabetes-induced change was absent in $Rho^{-/-}$ mice. Retinal gene expression of VEGF-A was significantly increased in WT mice with diabetes ($P < 0.05$), but was unchanged in $Rho^{-/-}$ mice. TNF-α gene expression significantly increased (4.9-fold) in WT mice with diabetes ($P < 0.05$) and also increased appreciably in $Rho^{-/-}$ mice but to a reduced extent (1.5 fold; $P < 0.05$). The outer nuclear layer in nondiabetic $Rho^{-/-}$ mice was reduced to a single layer after 6 months, but when diabetes was superimposed on this model, there was less degeneration of photoreceptors ($P < 0.05$). Vascular density was attenuated in diabetic WT mice compared with the nondiabetic control ($P < 0.001$); however, this diabetes-related disease was not observed in $Rho^{-/-}$ mice.

Conclusions. Loss of the outer retina reduces the severity of diabetic retinopathy in a murine model. Oxygen usage by the photoreceptors during dark adaptation may contribute to retinal hypoxia and exacerbate the progression of diabetic retinopathy. (*Invest Ophthalmol Vis Sci.* 2006;47:5561–5568) DOI:10.1167/iovs.06-0647

During diabetes, the cells of the retina and its microvasculature are exposed to sustained hyperglycemia-related biochemical stress and as a result suffer progressive dysfunction leading to premature death. Although the pathogenic basis of this vasodegenerative phase of diabetic retinopathy remains equivocal, the clinical characteristics and histopathology are well characterized and include basement membrane (BM) thickening, microaneurysm formation, excessive vasopermeability, pericyte/endothelial cell death, and, eventually, nonperfusion of microvascular segments in the inner retina.[1–3] Widespread capillary closure leads to substantial areas of inner retinal ischemia and the associated hypoxia precipitates inappropriate expression of angiogenic and vasopermeabilizing growth factors and elaboration of sight-threatening new vessels or macular edema in a significant proportion of patients.

There is increasing evidence that diabetic patients who also have the outer retinal degenerative disorder retinitis pigmentosa (RP) have a reduced risk of the development of preproliferative diabetic retinopathy.[4,5] Independently, diabetes and RP are relatively common in the population, although the occurrence of both diseases together is rare. Nevertheless, it has been recognized that RP correlates negatively with the severity of diabetic retinopathy.[6] Significantly, a study by Arden[5] of approximately 50 patients with RP who had been diabetic for a mean of ~40 years showed that none had microaneurysms, exudates, or other indicators of clinical diabetic retinopathy, even though they had other, nonretinal vascular complications associated with long-term diabetes. Furthermore, in an investigation employing the murine model of oxygen-induced retinopathy, the characteristically aggressive retinal neovascularization (NV) failed to appear when induced in mice modeling RP ($pdeb^{-/-}$). The same study reported spontaneous regression of retinal NV in diabetic patients after manifestation of clinically recognizable RP.[7]

It has been proposed that loss of rod photoreceptors during RP leads to a net reduction in oxygen usage by the retina,[8,9] a phenomenon that is intimately related to the high oxygen demands of these cells in combination with the dark adaptation response. During dark adaptation, the rod cells recover their high internal Ca^{2+} levels via cGMP-gated channels. This also accompanies influx of sodium ions and water that are subsequently removed from the rod cytoplasm, which is a heavily adenosine triphosphate (ATP)-dependent process that leads to the photoreceptor cell's consuming up to four times more oxygen than during light adaptation.[10] Even in the healthy retina, this dark cycle has been shown to result in a

From the [1]Centre for Vision Science, Queens University Belfast, Institute of Clinical Science Block A, Royal Victoria Hospital, Belfast, Northern Ireland; and [2]The Ocular Genetics Unit, Smurfit Institute, Department of Genetics, Trinity College Dublin, Dublin, Ireland.

Supported by Action Medical Research (UK) and the Juvenile Diabetes Research Fund (USA).

Submitted for publication June 14, 2006; revised August 1, 2006; accepted September 22, 2006.

Disclosure: **T.E. de Gooyer**, None; **K.A. Stevenson**, None; **P. Humphries**, None; **D.A.C. Simpson**, None; **T.A. Gardiner**, None; **A.W. Stitt**, None

The publication costs of this article were defrayed in part by page charge payment. This article must therefore be marked "*advertisement*" in accordance with 18 U.S.C. §1734 solely to indicate this fact.

Corresponding author: Alan W. Stitt, Centre for Vision Science, Queen's University Belfast, Royal Victoria Hospital, Grosvenor Road, Belfast BT12 6BA, Northern Ireland; a.stitt@qub.ac.uk.

relatively hypoxic condition, with corresponding changes in hypoxia-related transcriptional activity and growth factor gene expression.[11] Retinal hypoxia may be exacerbated in diabetic patients in whom the retina becomes increasingly hypoxic due to blood flow abnormalities, nonperfusion, and progressive ischemia. Indeed, the oxygen deficit experienced during diabetic retinopathy has been demonstrated using microelectrodes to measure Po_2 directly in the feline retina after long-term (~6-year duration) diabetes, and this deficit correlates with vascular disease.[12]

In a parallel study, we have reported that rhodopsin knockout mice with outer retinal degeneration show decreased hypoxia and that such changes can be replicated in normal animals by extended exposure to photoptic conditions or the use of a calcium channel blocker during dark adaptation.[11] Arden[5] has proposed that loss of rod cells during RP may offset the exacerbation of hypoxia during diabetic retinopathy and thereby protect the microvasculature from pathogenic change,[5] although this must be established experimentally in appropriate model systems. In the present investigation, experimental diabetes was superimposed on a transgenic murine model of RP with results that provide insight into both conditions.

METHODS

Experimental Model

The rhodopsin knockout mouse ($Rho^{-/-}$) displays a retinitis pigmentosa (RP)-like phenotype with progressive, age-dependent decline in rod number and function.[13] These animals display a reduced outer nuclear layer thickness and no rod ERG response at 48 days of age, with virtually complete rod photoreceptor loss by 3 months.[13]

Male $Rho^{-/-}$ and C57Bl/6 (wild-type; WT) mice weighing 20 to 25 g (5–6 weeks old) were randomly assigned to nondiabetic control or diabetic groups. Diabetes was induced by a single intraperitoneal injection of streptozotocin (STZ; Sigma-Aldrich, St. Louis, MO) at 180 mg/kg body weight,[14] whereas control animals received an equivalent dose of the drug vehicle (citrate buffer at pH 4.6). Mice were caged in pairs and allowed food and water ad libitum. Blood glucose levels in the diabetic groups were measured biweekly, and animals with levels greater than 20 mM were included in the study. All animals were killed at 5 months' duration of diabetes after at least 4 hours of light illumination, and the body weight was recorded. At postmortem, 50 μL of whole blood was collected in potassium-EDTA microvette tubes (Sarstedt, Nümbrecht, Germany) for subsequent analysis of glycated hemoglobin. The eyes were enucleated and the retinas prepared as detailed later. Eyes for histologic and immunohistochemical studies were fixed in freshly prepared 4% paraformaldehyde (PFA) in 0.1 M phosphate buffer (pH 7.4) and processed for paraffin embedding.

All procedures were in accordance with the U.K. Home Office Animals (Scientific Procedures) Act 1986, and conform to the ARVO Statement for the Use of Animals in Ophthalmic and Vision Research.

Measurement of Retinal Carboxymethyl-Lysine

For quantification of CML content, retinal samples were subjected to ultrasonic disruption in RIPA buffer. After centrifugation to remove tissue debris, the protein content of the resultant supernatant was measured with a bicinchoninic acid (BCA) protein assay kit (Pierce, Rockford, IL). Fifty microliters of sample (concentration: μg/mL) or advanced glycation end product (AGE)-BSA standard (0–200 μM) diluted in 0.05% Tween 20 and 0.2% BSA in 75 mM PBS were aliquoted in duplicate into a plate (Nunc C96 Maxisorp; eBioscience, San Diego, CA) that had been precoated with solid-phase antigen (1 μg/mL AGE-BSA in 0.05 M carbonate buffer [pH 9.6]) overnight at 4°C and blocked with 3% skim milk powder for 1.5 hours. Fifty microliters of 1:2000 rabbit polyclonal anti-CML antibody (gift from Suzanne Thorpe, Department of Chemistry and Biochemistry, University of South Carolina, Columbia, SC) was added to sample and standard wells, and plates were incubated for 2 hours at room temperature. Wells containing 100 μL of diluting buffer were used as a nonsample, nonantibody blank. Plates were washed in buffer (0.2 mM KH_2PO_4, 1.4 mM K_2HPO_4, 3 mM NaCl, 0.45 μM sorbic acid potassium, and 0.01% Tween-20) using an ELISA plate washer (3 × 300 μL) and 100 μL of peroxidase-conjugated anti-rabbit IgG (diluted 1:5000 in 0.1% BSA in PBS; Sigma-Aldrich) was added to each well and incubated for 1 hour at room temperature. Plates were again washed before the color reaction was started by the addition of 150 μL of tetramethyl-benzine substrate (TMB; Sigma-Aldrich) to each well. The reaction was stopped after 30 minutes by the addition of 50 μL of 2 M sulfuric acid, and the absorbance of the blue reaction product was measured at 450 nm on a microplate reader (Safire; Tecan Instruments, Switzerland). Results (minus blank absorbance) were expressed as a percentage of the zero standard (nonsample, antibody control) and CML concentration in samples determined by comparison to the standard curve.

Determination of Retinal Hypoxia

Retinal hypoxia can be immunolocalized and quantified using the bioreductive drug pimonidazole,[15] which forms irreversible adducts with thiol groups on tissue proteins when Po_2 is less than 10 mm Hg.[16] Mice with diabetes of 5 months' duration or age matched control mice (n = 6–9 animals/group) were administered 60 mg/kg pimonidazole (Hypoxyprobe; HP; Chemicon Europe Ltd., Chandlers Ford, UK) in sterile water by intraperitoneal injection. After 3 hours, animals were killed, and eyes were enucleated. The right eye was fixed in 4% PFA for 4 hours then placed in PBS at 4°C for HP immunolocalization studies, whereas an incision was made in the left eye 2 mm posterior to the ora serrata, and the anterior segment, lens, and vitreous were removed before the retina was freshly dissected from the posterior eye cup and snap frozen in liquid nitrogen. Before HP quantification by indirect competitive ELISA, retinal weight was recorded by collecting tissues in preweighed tubes.

For quantification of HP-protein binding, preweighed retinal samples from diabetic and nondiabetic $Rho^{-/-}$ and WT mice were prepared for an HP competitive ELISA.[17] Snap-frozen retinas were subjected to ultrasonic disruption in RIPA buffer. After centrifugation to remove tissue debris, the protein content of the resultant supernatant was measured in a BCA protein assay kit (Pierce). One hundred microliters of sample (45 μg/mL) or standard (0–20 μM) diluted in PBS/5% Tween 20 were aliquoted in duplicate into a 96-well polystyrene assay plate (Corning-Costar Inc., Corning, NY) and incubated with 25 μL of rabbit polyclonal antibody against HP (1:3300 in PBS/5% Tween; kindly donated by James A. Raleigh, University of North Carolina School of Medicine, Chapel Hill, NC) for 1 hour at 37°C. The contents of each well was then transferred to plates (Nunc C96 Maxisorp; eBioscience) that had been precoated with solid phase antigen (1:5000 in carbonate buffer [pH 9.6]) overnight at 4°C and blocked with 1% gelatin for 1 hour. The competition between solid-phase (HP reductively bound to bovine serum albumin[17]) and soluble antigens proceeded for 1 hour at 37°C, after which the wells were washed four times for 5 minutes each with PBS/5% Tween, and 100 μL of 1:2000 alkaline-phosphatase goat anti-rabbit IgG (Sigma-Aldrich) was added to each well. Plates were then washed four times for 5 minutes each with PBS/5% Tween, and 100 μL of 1 mg/mL of the alkaline-phosphatase substrate, 4-nitrophenyl phosphate disodium salt hexahydrate (Sigma-Aldrich) dissolved in 10% diethanolamine buffer (pH 9.6) was added to each well. The color development of the subsequent reaction was measured at 405 nm every 5 minutes for 2 hours on a microplate reader (Safire; Tecan Instruments), and the reaction kinetics were analyzed (Magellan ver. 3.11 software; Tecan Instruments). Sample HP binding was determined by comparison to a Lineweaver-Burk enzyme kinetic standard curve and is expressed as a proportion of sample protein concentration and corrected for retinal tissue weight.

For HP-immunolocalization, randomly chosen 5-μm paraffin-embedded sections of 4% PFA-fixed eyes were dewaxed and rehydrated in graded alcohols and tap water. Sections were then incubated with a 1:1

solution of trypsin and versene (DIFCO, Detroit, MI) to unmask antigenic regions, washed in distilled H_2O for 10 minutes, and incubated for 20 minutes in PBS containing 0.1% Triton X-100 (TX-100) to permeabilize the tissue, and 10% normal goat serum to block nonspecific binding of the primary antibody. For visualization of the HP-protein adducts, sections were incubated with an anti-HP rabbit polyclonal antibody used at a dilution of 1:500 in PBS/0.1% TX-100, overnight at 4°C. For secondary detection, sections were washed three times in 5-minute changes of PBS, and covered in a 1:200 dilution in PBS/0.1% TX-100 of a goat anti-rabbit antibody labeled with Alexa-488 (Invitrogen-Molecular Probes Europe BV, Leiden, The Netherlands) for 1 hour at room temperature. Sections were again washed three times in 5-minute changes of PBS, covered with 5 nM of propidium iodide (Sigma-Aldrich) in PBS/0.1% TX-100 for 20 minutes at room temperature to visualize cell nuclei, and further washed in PBS for 15 minutes before being mounted (Vectashield; Vector Laboratories Ltd., Peterborough, UK).

Quantitative RT-PCR

Freshly dissected mouse retinas ($n = 6–8$) were snap frozen in liquid nitrogen. RNA was extracted with (Tri-reagent; Sigma-Aldrich) according to the manufacturer's instructions, and purified (RNeasy Mini Kit; Qiagen, Crawley, UK) with residual DNA removed by DNase I digestion (Qiagen). The quantity of RNA in each sample was determined spectrophotometrically (NanoDrop Technologies, LabTech International, Ringmer, UK). RNA samples were reverse transcribed into cDNA (Superscript II RNase H^- reverse transcriptase; Invitrogen, Paisley, UK), with a first-strand cDNA synthesis kit (Invitrogen-Life Technologies) and random hexamer primers (Roche Molecular Biochemicals, Mannheim, Germany). Real-time reverse transcription-PCR (RT-PCR) was conducted for quantitative analysis of mRNA expression using murine sequence-specific primers. For normalization of expression data, a 100-bp fragment of 28s (forward: 5′ TTG AAA ATC CGG GGG AGA G 3′, reverse: 5′ ACA TTG TTC CAA CAT GCC AG 3′) was amplified. Primers used to amplify further murine genes were: the rod photoreceptor specific cGMP phosphodiesterase (PDE6b; forward: 5′ TAC CAC AAC TGG CGC CAC 3′, reverse: 5′ GTA ACC ATG GGC AAG GCC 3′, 110-bp fragment); VEGF-A (forward: 5′ TTA CTG CTG TAC CTC CAC C 3′; reverse: 5′ ACA GGA CGG CTT GAA GAT G 3′, 189-bp fragment); tumor necrosis factor (TNF)-α (forward: 5′ GAC CCT CAC ACT CAG ATC ATC TTC 3′, reverse: 5′ CGC TGG CTC AGC CAC TCC 3′, 104-bp fragment)[18]; collagen IV (forward: 5′ GGT GTC AGC AAT TAG GCA GGT CAA G 3′, reverse: 5′ ACT CCA CGC AGA GCA GAA GCA AGA A 3′, 263-bp fragment)[19]; and laminin β1 (forward: 5′ AGC AGA AAA GGC CCA GGT 3′, reverse: 5′ GGT TTC CTC AGA AGC TGC 3′, 118-bp fragment).

Real-time RT-PCR was performed with a rapid thermal cycler system (LightCycler; Roche Molecular Biochemicals), according to protocols outlined by Simpson et al.[20] and Feeny et al.[21] Briefly, PCR was performed in glass capillary reaction vessels (Roche Molecular Biochemicals) in a 10-μL volume with 0.5 μM primers. Reaction buffer, 2.5 mM $MgCl_2$, dNTPs, *Taq* DNA polymerase (Hotstart), and green fluorescent dye (SYBR Green I) were included in a kit (QuantitTect LightCycler, SYBR Green PCR Master Mix; Qiagen, Crawley, UK). Amplification of cDNAs involved a 15-minute denaturation step followed by 40 cycles with a 95°C denaturation for 15 seconds, 50°C to 60°C annealing for 20 seconds, and 72°C appropriate extension time (10–15 seconds). Fluorescence from the green dye that bound to the PCR product was detected at the end of each 72°C extension period. The specificity of the amplification reactions was confirmed by melting-curve analysis.[20] The quantification data were analyzed with the analysis software that accompanied the thermal cycler (Light Cycler; Roche Molecular Biochemicals), as described previously.[22] Background fluorescence was removed by setting a noise band on a plot of log fluorescence against cycle number. The number of cycles at which the best-fit line through the log-linear portion of each amplification curve intersects the noise band is inversely proportional to the log of the copy number.[23] A dilution series of a reference cDNA sample was used to generate a standard curve against which the experimental samples were quantified. For each gene, PCR amplifications were performed in triplicate on at least two independent RT reactions.

As the outer retina is lost in the $Rho^{-/-}$ mice, the relative contribution that these cells make differs compared with WT. The total amount of RNA recovered per retina in $Rho^{-/-}$ was consistently lower than WT and decreased as outer retinal degeneration progressed.[11] To account for the uneven contribution that the inner retina would be making to the measurement of gene expression, after normalization to 28s, $Rho^{-/-}$ expression results were also divided by the factor difference of the RNA concentration compared with WT.

ADPase Enzyme Histochemistry

Evaluation of the retinal vasculature according to adenosine diphosphatase (ADPase) activity in whole embedded retina was performed according to the methodology described in detail by Lutty and McLeod.[24] As a retinal vessel visualization technique, this approach has been extensively used in experimental diabetes investigations.[25,26] After overnight fixation of intact eyes in 2% PFA in 0.1 M cacodylate buffer at 4°C, an incision was made 2 mm posterior to the ora serrata, and the anterior segment of the eye was removed. After the vitreous was removed from the eye cup, the retina was carefully separated from the RPE and choroid, washed in 0.1 M cacodylate buffer with 5% sucrose, and incubated for enzyme histochemical demonstration of ADPase activity. The ADPase-incubated retina was washed in 0.1 M cacodylate buffer with 5% sucrose, and four radial cuts were made from the retinal periphery to points within 1 mm from the optic disc, to relax the retina before flat fixation in one-fourth strength Karnovsky's buffer for 72 hours. After 3 brief washes in 0.1 M cacodylate buffer with 5% sucrose, the fixed retinas were dehydrated in graded alcohols and flat embedded in resin (JB4; PolySciences Europe, Eppelheim, Germany). Retinal microvascular density was quantified using Image J software (ver. 1.30; available by ftp at http://rsb.info.nih.gov/nih-image; developed by Wayne Rasband, National Institutes of Health, Bethesda, MD) on ADPase-labeled flatmounts. A minimum of four fields of view were quantified from each retina in a blinded fashion from a minimum of $n = 6$ mice.

Evaluation of Outer Retinal Morphology

To evaluate the effect of diabetes on photoreceptor degeneration in $Rho^{-/-}$ mice, eyes from control and diabetic mice were fixed in 4% PFA for 4 hours and washed in PBS before dehydration and embedding in wax for sectioning at 5 μm. Four randomly chosen sections from at least six retinas were dewaxed, rehydrated, stained with 5 nM propidium iodide (Sigma-Aldrich) for 20 minutes, washed for 15 minutes in PBS/0.1% Triton X-100, and mounted (Vectashield; Vector Laboratories). Three images were captured of the central and peripheral regions of the retina with a fluorescence microscope (BX60; Olympus UK Ltd., London, UK) fitted with a confocal scanning laser microscope (MicroRadiance; Bio-Rad, Herts, UK). Images were opened on computer (Photoshop; Adobe Systems, San Jose, CA), a box of consistent dimensions was overlaid, and the number of nuclei per area was counted in sections by an observer masked to the conditions of the eyes from which they were obtained.

Statistical Analysis

Data were analyzed (Instat; GraphPad Software Inc., San Diego, CA), with one-way analysis of variance (ANOVA) conducted among three or more groups, with post hoc analysis made with the Tukey-Kramer multiple comparisons test. Statistical comparison of data between two groups was made with a *t*-test for independent samples. $P < 0.05$ was considered statistically significant.

Results

An overview of glycemic control and weight gain is presented in Table 1. Diabetic animals had significantly lower body

weights than their nondiabetic counterparts ($P < 0.01$). Glycated hemoglobin as a intermediate-term measure of glycemia was significantly altered in the diabetic animals compared with the nondiabetics, irrespective of whether they were WT or Rho$^{-/-}$ ($P < 0.001$). As a long-term indicator of glycemia, the AGE CML has been shown to be elevated in diabetic retinas,[27] and in the present study, ELISA quantification of CML immunoreactivity in the retina was significantly increased in WT diabetic compared with nondiabetic animals (5.412 ± 0.017 vs. 4.16 ± 0.038 μg/retina; $P < 0.05$). This trend was reversed in the Rho$^{-/-}$ group, with higher levels of CML immunoreactivity apparent in nondiabetic groups than in the diabetic group (4.488 ± 0.048 vs. 2.514 ± 0.018 μg/retina; $P < 0.05$).

Hypoxia, as indicated by HP adduct deposition, was markedly increased in retina from WT animals with 5-month diabetes duration, when compared with nondiabetic control mice (compare Fig. 1A with 1B). Most of the HP immunoreactivity in diabetic retinas was within the inner retinal neurons, especially in the ganglion cell layer (GCL) and around cells in the inner nuclear layer (INL), possibly Müller glia cell bodies (Fig. 1B). In nondiabetic retinas, there was low-level HP immunoreactivity in the GCL that was completely absent in the INL (Fig. 1A). In the Rho$^{-/-}$ mouse retina, most of the HP deposition occurred in the GCL with less fluorescence intensity in the diabetic Rho$^{-/-}$ mice (compare Figs. 1C and 1D). Qualitative assessment was confirmed via ELISA quantification of HP adduct retinal extracts, with significantly more hypoxia in WT diabetic than in nondiabetic counterparts ($P < 0.001$; Fig. 1E). Retina from diabetic Rho$^{-/-}$ mice had significantly less HP deposition when compared with WT diabetic retina ($P < 0.001$; Fig. 1E).

Analysis of mRNA expression, as determined by real-time RT-PCR, revealed that the mRNAs encoding the BM component proteins laminin β1 and collagen IV were upregulated by diabetes in WT animals ($P < 0.05$), as previously shown[27]; Rho$^{-/-}$ mice failed to show this characteristic diabetes-related response (Fig. 2). Similarly, mRNA encoding the hypoxia-regulated growth factor VEGF-A was significantly upregulated in diabetic retina compared with nondiabetic ($P < 0.05$), although this alteration was not observed in Rho$^{-/-}$ animals (Fig. 3A). TNF-α mRNA expression was increased in WT mice with diabetes, and this trend was also evident in diabetic Rho$^{-/-}$ mice, although to a lesser extent (Fig. 3B).

Retinal morphology was assessed in sections, and outer retinal degeneration was quantified by counting nuclei at the level of the outer retina juxtaposed to the RPE and INL. Nondiabetic Rho$^{-/-}$ animals showed the expected depletion of photoreceptor cell nuclei at 5 months; however, their diabetic counterparts showed a significant survival of photoreceptors in both the peripheral and central retina ($P < 0.05$; Fig. 4). This was also confirmed by quantitative analysis of PDE6b mRNA expression, with a significant residual level of expression of this photoreceptor-specific gene retained in the diabetic Rho$^{-/-}$ animals. There was no difference in photoreceptor cell survival between WT normal and diabetic groups (Fig. 4).

Table 1. Metabolic Parameters in Control and Diabetic WT and Rho$^{-/-}$ Mice

	Body Weight (g)	% GHb
WT Control	35.3 ± 0.7	7.3 ± 0.3*
WT Diabetic	23.0 ± 0.7	15.3 ± 0.6†
Rho$^{-/-}$ Control	35.4 ± 0.9	6.8 ± 0.3*
Rho$^{-/-}$ Diabetic	24.1 ± 0.9	16.3 ± 0.4†

For the duration of the diabetes study (5 months), both groups of diabetic mice showed comparable, elevated levels of glycated Hb and associated weight loss.

* $P < 0.01$, body weight between diabetic and nondiabetic mice.

† $P < 0.001$, HbA1c between diabetic ad nondiabetic mice.

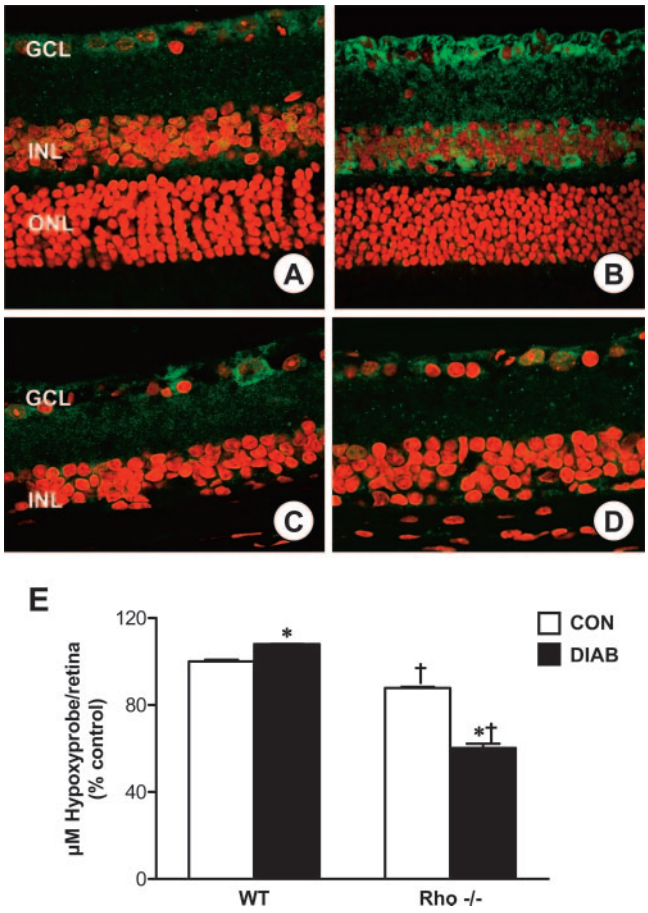

Figure 1. Hypoxia in retina during diabetes and rod photoreceptor depletion. Pimonidazole (Hypoxyprobe; Chemicon Europe, Ltd.) immunoreactivity is shown as *green* fluorescence by confocal microscopy. Nuclei of retinal cells are counterstained with propidium iodide (*red* fluorescence). The WT retina show HP deposition at the level of the ganglion cell layer (**A**), whereas HP staining intensity is increased in diabetes (**B**), appearing in cells within the INL. Overall, HP-immunoreactivity is reduced in WT Rho$^{-/-}$ retina (**C**), and this is further reduced in the presence of diabetes (**D**). Qualitative assessment was confirmed using the quantitative HP-ELISA (**E**). Results are expressed as the mean ± SEM. *$P < 0.001$, diabetic compared with the nondiabetic control; †$P < 0.001$, Rho$^{-/-}$ compared with WT.

Retinal microvascular density in ADPase-stained retinal flatmounts was quantified, and there was a significant reduction in capillary density in diabetic WT mice when compared with the control ($P < 0.001$; Fig. 5). In the Rho$^{-/-}$ retinas, the vascular tree was less dense overall when compared with WT (as has been previously shown[11]); however, the diabetic Rho$^{-/-}$ mice appeared to have lost fewer capillaries than had their nondiabetic counterparts ($P < 0.001$; Figs. 5C, 5D). Also, in the context of diabetes, there was a significant increase in vascular density in the Rho$^{-/-}$ mice when compared with the WT diabetic counterparts ($P < 0.05$; Figs. 5B, 5D).

Discussion

There is enhanced oxygen usage by rod photoreceptors under scotopic conditions, and, in some disease states, this physiological phenomenon could serve to exacerbate pathologic hypoxia.[10,28] It has been suggested that photoreceptor metabolism could play a contributory role in initiation and progression of

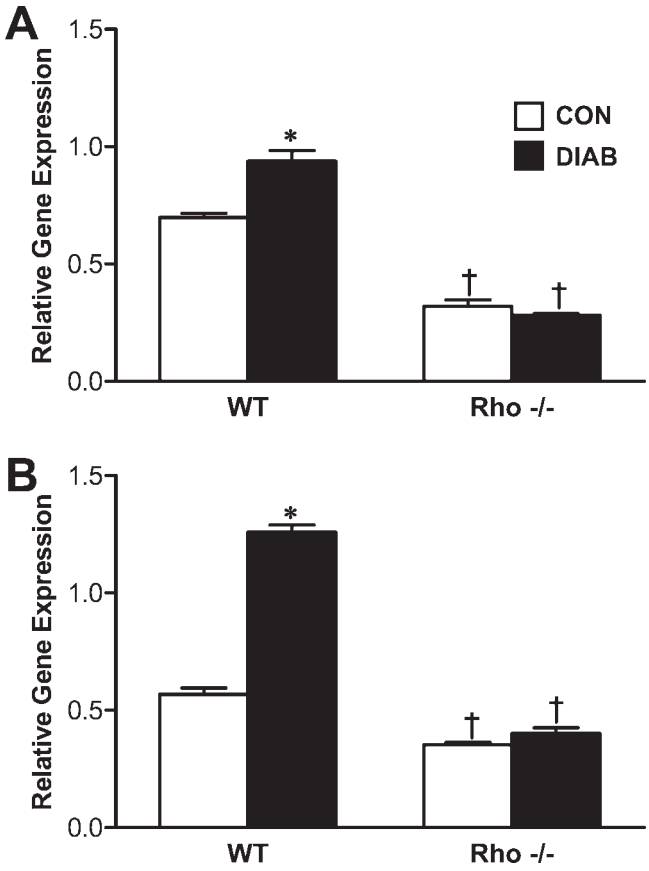

FIGURE 2. BM component mRNAs were increased in WT diabetic but not in Rho$^{-/-}$ diabetic retinas. BM thickening is a characteristic of diabetic retinopathy and alterations in BM component mRNAs have been shown to be a reliable surrogate marker of BM thickening in the diabetic retina. As has been demonstrated, laminin β1 (**A**) and collagen IV (**B**) mRNAs were increased in the presence of 5 months of diabetes in WT mice by real-time RT-PCR. This increase was not observed in the Rho$^{-/-}$ retina (**A**, **B**). Results are expressed as the mean ± SEM. *$P <$ 0.05, diabetic compared with the nondiabetic control; †$P < 0.05$, Rho$^{-/-}$ compared with WT.

diabetic retinopathy even before there is overt microvascular damage.[5,7] In a parallel investigation to the present study we have shown that Rho$^{-/-}$ mice demonstrate less retinal hypoxia than do wild-type counterparts and that relative hypoxia in normal retina was reduced when WT mice were kept in photopic conditions or treated with the cGMP-blocker L-*cis*-diltiazem.[11] This indicates a direct role of photoreceptor metabolism on retinal oxygen usage.[11]

It is widely accepted that the human retina experiences progressive vascular insufficiency during diabetes, culminating in overt ischemia that may drive an aggressive NV response and/or macular edema. The role for hypoxia in this disease has been shown indirectly by measuring growth factors like VEGF, the levels of which appear highest in the proliferative phase of the disease.[29–31] Most animal models of diabetic retinopathy do not show the widespread ischemia experienced by long-term diabetic patients, and it often takes more than 5 months of experimental diabetes to show a relatively meager threefold increase in acellular capillaries.[27,32] Nevertheless, this progressive vascular insufficiency is often associated with increases in retinal VEGF.[33,34] In the diabetic cat, relative retinal hypoxia occurs even in the absence of widespread nonperfusion, as demonstrated by direct (microelectrode) Po_2 measurements.[12] In the present study, STZ-induced diabetes produced relative hypoxia after 5 months of diabetes, and this effect is probably related to the gradual depletion of microvasculature which may account for progressive increases in VEGF expression.

An important finding in the current investigation has been that diabetic Rho$^{-/-}$ mice suffer proportionately less retinal hypoxia and reduced pathologic symptoms when compared with their diabetic WT counterparts. According to our to HP immunolocalization studies, most of the hypoxia was experienced by the innermost layers of the retina during diabetes, specifically in the ganglion cells and to a lesser extent, the Müller glia. Ganglion cells and Müller glia are important sources of angiogenic growth factors in the retina, including VEGF,[30,35,36] and these cells show dysfunction during hyperglycemia and hypoxia.[37] It is interesting that ganglion cells deposit the greatest levels of HP, and these cells may suffer most from fluctuations in hypoxia. We have previously demonstrated that neither Müller glia nor astrocytes deposit HP in overly ischemic retina,[15] but in the diabetic context, where vascular insufficiency is more subtle, HP is pronounced in the Müller glia when compared with that in the nondiabetic retina. This may indicate chronic hypoxic load in these cells during diabetes, and this is also reflected by the metabolic switch shown in Müller glia in diabetic retina, where they derive much of their ATP from anaerobic glycolysis with less reliance on oxidative phosphorylation.[38]

Microvascular disease is reduced in the diabetic Rho$^{-/-}$ mouse retina when compared with WT that in the diabetic

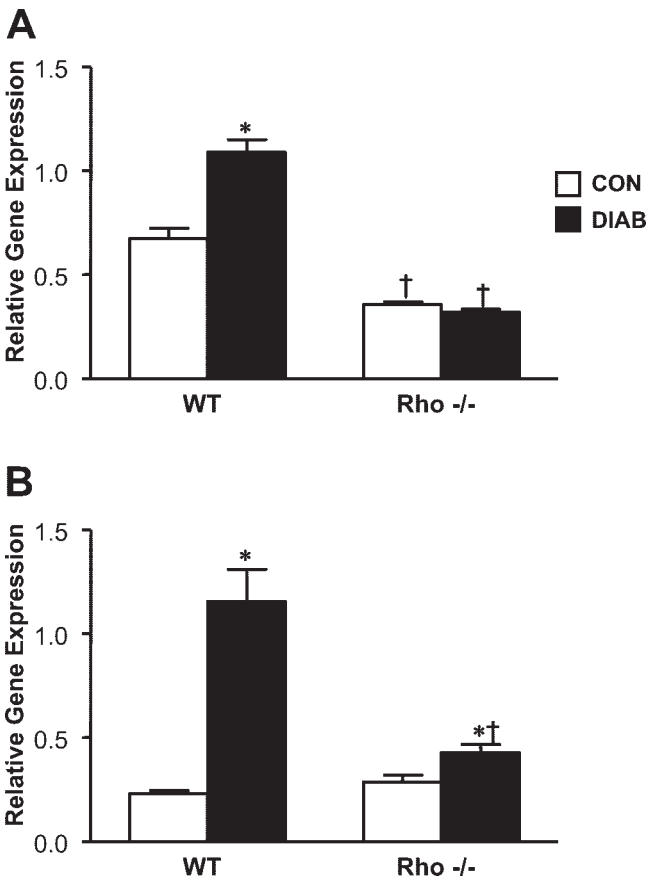

FIGURE 3. VEGF and TNF-α mRNAs were increased in WT diabetic but not in Rho$^{-/-}$ diabetic retinas. VEGF (**A**) and TNFα (**B**) expression, as assessed by real-time RT-PCR, was significantly increased in diabetes in the WT retina but this diabetes-mediated increase was not evident in the Rho$^{-/-}$ mice. Results are expressed as the mean ± SEM. *$P < 0.05$, diabetic compared with the nondiabetic control; †$P < 0.05$, Rho$^{-/-}$ compared with WT.

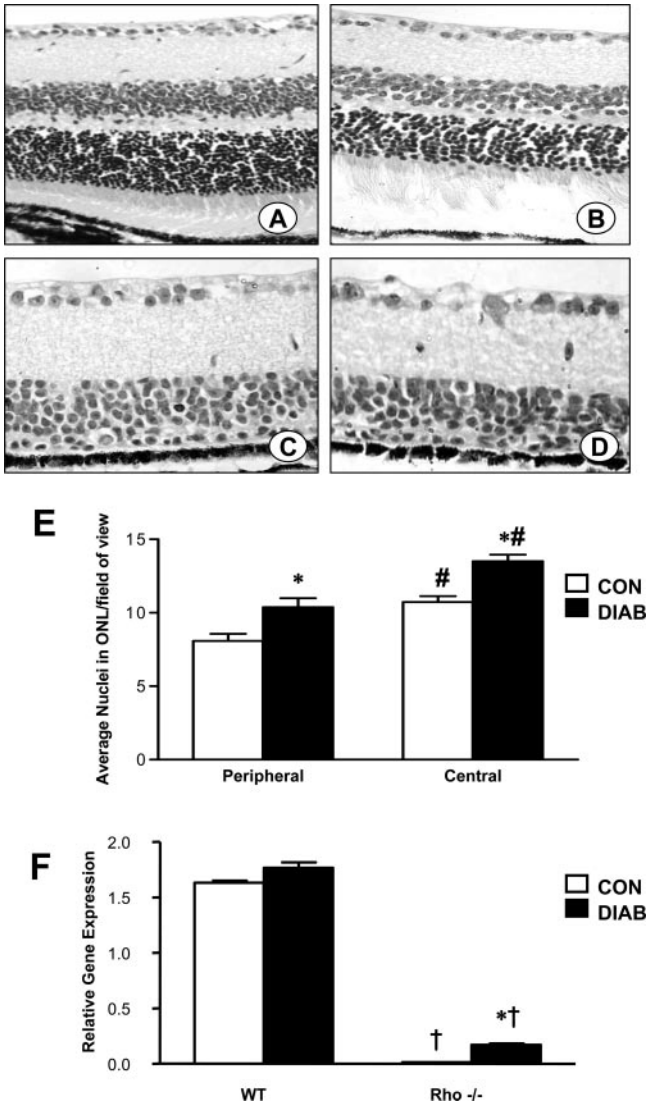

FIGURE 4. Photoreceptor loss in the Rho$^{-/-}$ retina was influenced by diabetes. Retinal morphology was assessed in sections from WT nondiabetic (**A**), WT diabetic (**B**), Rho$^{-/-}$ nondiabetic (**C**), and Rho$^{-/-}$ diabetic (**D**) mice. Using these sections, outer retinal degeneration was quantified by counting nuclei in the region once occupied by the ONL in both the peripheral and central retina from Rho$^{-/-}$ mice only (**E**). A parallel quantitative study assessed photoreceptor-specific PDE mRNA expression (**F**). Nondiabetic Rho$^{-/-}$ showed the almost complete loss of photoreceptor cell nuclei at 5 months (compare **A** with **C**); however, their diabetic counterparts showed a significant survival of photoreceptors in both the peripheral and central retina (**E**). This was also confirmed by quantitative analysis of PDE6b mRNA expression, with a significant residual level of expression of this photoreceptor-specific gene retained in the diabetic Rho$^{-/-}$ animals. There was no difference in photoreceptor cell survival between the WT normal and diabetic groups. Results are expressed as the mean ± SEM. *$P < 0.05$, diabetic compared with the nondiabetic control; †$P < 0.05$, Rho$^{-/-}$ compared with WT; #$P < 0.05$, central compared with peripheral retina.

mouse. The retinal microvasculature of the Rho$^{-/-}$ mouse is already significantly depleted compared with WT animals at 5 months, but it is important to note that there is still considerable vessel density remaining in the Rho$^{-/-}$ retina at 5 months. In these mice, the presence of diabetes causes no further vessel attenuation, which contrasts markedly with the response to diabetes in the WT mouse. The protection against retinopathy is further reinforced by the mRNA expression data, which show that VEGF and TNF-α are significantly upregulated in diabetic WT mice compared with nondiabetic control mice but that this difference is lost with photoreceptor degeneration. Furthermore, upregulation of BM component mRNAs (a surrogate indicator of retinal microvascular BM thickening in diabetic rodents[27]) is also absent in the presence of photoreceptor degeneration. The link between retinal hypoxia and BM remodeling and thickening is not established in the retina, although there is evidence that hypoxia stimulates TGF-β1–mediated upregulation of BM components in many organs including skin,[39] kidney,[40] and lung.[41] It remains possible that a similar phenomenon occurs in the diabetic retina.

This investigation has shown that diabetes is associated with increased survival of the photoreceptor cells in Rho$^{-/-}$ mice as indicated by more photoreceptor nuclei in the ONL and a significantly higher level of PDE mRNA expression compared than in nondiabetic counterparts. Why diabetes should reduce photoreceptor loss in this RP model is unknown, and

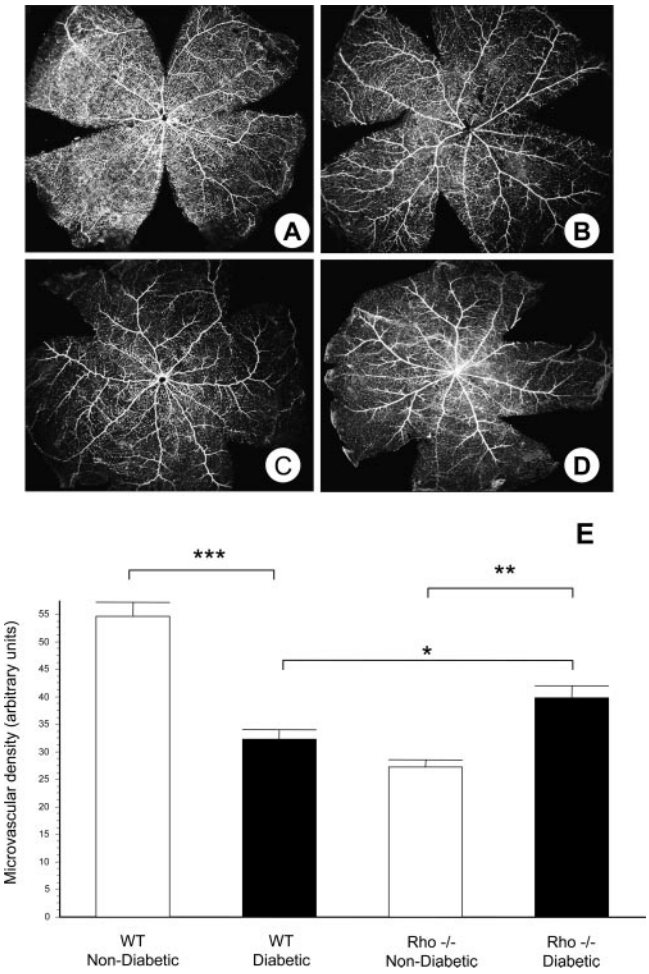

FIGURE 5. Microvascular density in diabetic WT and Rho$^{-/-}$ retina. The retinal microvasculature was assessed by ADPase enzyme histochemistry in retinas from nondiabetic WT (**A**), diabetic WT (**B**), nondiabetic Rho$^{-/-}$ (**C**), and diabetic Rho$^{-/-}$ (**D**) mice. Dark-field images show vascular density in the mid and peripheral regions of flat-mounted, embedded retinas. Quantification shows that in contrast to the dense vascular tree of the WT, retina from the Rho$^{-/-}$ had vascular attenuation in the capillary beds (**E**). There was a significant loss of vasculature during 5 months of diabetes, but this acellular capillary formation was not observed in diabetic Rho$^{-/-}$ mice (**E**). There was significantly less depletion in the Rho$^{-/-}$ diabetic retinas when compared with their nondiabetic counterparts. The results are expressed as the mean ± SEM. *$P < 0.05$; **$P < 0.01$; ***$P < 0.001$).

these data contrast with recent studies that indicate a modest reduction in ONL thickness in diabetic mice[42] and rats.[43] There is also evidence of reversible alterations in the electroretinogram (ERG),[44,45] defects in color perception,[46] and impaired contrast sensitivity[47] in diabetic patients and animal models. Within the context of the present study, it is likely that the acute and widespread photoreceptor apoptosis occurring in $Rho^{-/-}$ mice is distinct from the sporadic depletion of neurons throughout the full-thickness retina during long-term diabetes. Moreover, it is interesting that exposure to high-glucose conditions may actually inhibit apoptosis through enhanced expression of the anti-apoptotic proteins Bcl-2 and Bcl-xl.[48] These proteins are expressed in photoreceptors,[49] and upregulation of Bcl-2 in these cells can protect against apoptotic death in a murine model of RP.[50]

The present study has added support to the hypothesis that oxygen usage by the ONL may have a profound impact on the retina during certain disease conditions by regulating hypoxia-linked gene expression. It has been demonstrated that rod photoreceptor metabolism during scotopic conditions may exacerbate the hypoxic load experienced in disorders such as diabetic retinopathy in which a progressive microvascular insufficiency is occurring. It is possible that agents or therapeutic regimens that modulate photoreceptor oxygen usage without interfering with visual function, possibly L-*cis*-diltiazem, which is widely used clinically, could have a beneficial impact on the progression of diabetic retinopathy. This assertion is also supported by findings in a separate murine model of RP ($pdeb^{-/-}$) incorporated into the oxygen-induced retinopathy (OIR) regimen, in which there is also significantly reduced ischemia-induced preretinal neovascularization.[7] These outcomes are informative about the role of relative hypoxia in the retina, its link to pathogenicity, and how this fine balance between oxygen influx and usage can be upset during disease.

Acknowledgments

The authors thank Mathew Owens for technical support.

References

1. Hammes HP. Pericytes and the pathogenesis of diabetic retinopathy. *Horm Metab Res*. 2005;37(suppl 1):39–43.
2. Lorenzi M, Gerhardinger C. Early cellular and molecular changes induced by diabetes in the retina. *Diabetologia*. 2001;44:791–804.
3. Fong DS, Aiello L, Gardner TW, et al. Retinopathy in diabetes. *Diabetes Care*. 2004;27(suppl 1):S84–S87.
4. Arden GB, Wolf JE, Tsang Y. Does dark adaptation exacerbate diabetic retinopathy?—evidence and a linking hypothesis. *Vision Res*. 1998;38:1723–1729.
5. Arden GB. The absence of diabetic retinopathy in patients with retinitis pigmentosa: implications for pathophysiology and possible treatment. *Br J Ophthalmol.* 2001;85:366–370.
6. Sternberg P Jr., Landers MB 3rd, Wolbarsht M. The negative coincidence of retinitis pigmentosa and proliferative diabetic retinopathy. *Am J Ophthalmol*. 1984;97:788–789.
7. Lahdenranta J, Pasqualini R, Schlingemann RO, et al. An anti-angiogenic state in mice and humans with retinal photoreceptor cell degeneration. *Proc Natl Acad Sci USA*. 2001;98:10368–10373.
8. Penn JS, Li S, Naash MI. Ambient hypoxia reverses retinal vascular attenuation in a transgenic mouse model of autosomal dominant retinitis pigmentosa. *Invest Ophthalmol Vis Sci*. 2000;41:4007–4013.
9. Arden GB, Sidman RL, Arap W, Schlingemann RO. Spare the rod and spoil the eye. *Br J Ophthalmol*. 2005;89:764–769.
10. Braun RD, Linsenmeier RA, Goldstick TK. Oxygen consumption in the inner and outer retina of the cat. *Invest Ophthalmol Vis Sci*. 1995;36:542–554.
11. de Gooyer TE, Stevenson KA, Humphries P, et al. Rod photoreceptor loss in $Rho^{-/-}$ mice reduces retinal hypoxia and hypoxia-related gene expression. *Invest Ophthalmol Vis Sci*. 2006;47:5553–5560.
12. Linsenmeier RA, Braun RD, McRipley MA, et al. Retinal hypoxia in long-term diabetic cats. *Invest Ophthalmol Vis Sci*. 1998;39:1647–1657.
13. Humphries MM, Rancourt D, Farrar GJ, et al. Retinopathy induced in mice by targeted disruption of the rhodopsin gene. *Nat Genet*. 1997;15:216–219.
14. Cox OT, Simpson DA, Stitt AW, Gardiner TA. Sources of pdgf expression in murine retina and the effect of short-term diabetes. *Mol Vis*. 2003;9:665–672.
15. Gardiner TA, Gibson DS, de Gooyer TE, de la Cruz VF, McDonald DM, Stitt AW. Inhibition of tumor necrosis factor-alpha improves physiological angiogenesis and reduces pathological neovascularization in ischemic retinopathy. *Am J Pathol*. 2005;166:637–644.
16. Raleigh JA, Koch CJ. Importance of thiols in the reductive binding of 2-nitroimidazoles to macromolecules. *Biochem Pharmacol*. 1990;40:2457–2464.
17. Raleigh JA, La Dine JK, Cline JM, Thrall DE. An enzyme-linked immunosorbent assay for hypoxia marker binding in tumours. *Br J Cancer*. 1994;69:66–71.
18. Lau J, Borjesson A, Holstad M, Sandler S. Prolactin regulation of the expression of TNF-alpha, IFN-gamma and il-10 by splenocytes in murine multiple low dose streptozotocin diabetes. *Immunol Lett*. 2006;102:25–30.
19. Nishikawa T, Giardino I, Edelstein D, Brownlee M. Changes in diabetic retinal matrix protein mRNA levels in a common transgenic mouse strain. *Curr Eye Res*. 2000;21:581–587.
20. Simpson DA, Feeney S, Boyle C, Stitt AW. Retinal VEGF mRNA measured by SYBR I green fluorescence: a versatile approach to quantitative PCR. *Mol Vis*. 2000;6:178–183.
21. Feeney SA, Simpson DA, Gardiner TA, Boyle C, Jamison P, Stitt AW. Role of vascular endothelial growth factor and placental growth factors during retinal vascular development and hyaloid regression. *Invest Ophthalmol Vis Sci*. 2003;44:839–847.
22. Morrison TB, Weis JJ, Wittwer CT. Quantification of low-copy transcripts by continuous SYBR green I monitoring during amplification. *BioTechniques*. 1998;24:954–958,960,962.
23. Higuchi R, Fockler C, Dollinger G, Watson R. Kinetic pcr analysis: Real-time monitoring of DNA amplification reactions. *BioTechnology (NY)*. 1993;11:1026–1030.
24. Lutty GA, McLeod DS. Phosphatase enzyme histochemistry for studying vascular hierarchy, pathology, and endothelial cell dysfunction in retina and choroid. *Vision Res*. 2005;45:3504–3511.
25. Johnson MA, Lutty GA, McLeod DS, et al. Ocular structure and function in an aged monkey with spontaneous diabetes mellitus. *Exp Eye Res*. 2005;80:37–42.
26. Kim SY, Johnson MA, McLeod DS, et al. Retinopathy in monkeys with spontaneous type 2 diabetes. *Invest Ophthalmol Vis Sci*. 2004;45:4543–4553.
27. Stitt A, Gardiner TA, Alderson NL, et al. The age inhibitor pyridoxamine inhibits development of retinopathy in experimental diabetes. *Diabetes*. 2002;51:2826–2832.
28. Yu DY, Cringle SJ, Su EN, Yu PK. Intraretinal oxygen levels before and after photoreceptor loss in the rcs rat. *Invest Ophthalmol Vis Sci*. 2000;41:3999–4006.
29. Adamis AP, Miller JW, Bernal MT, et al. Increased vascular endothelial growth factor levels in the vitreous of eyes with proliferative diabetic retinopathy. *Am J Ophthalmol*. 1994;118:445–450.
30. Gerhardinger C, Brown LF, Roy S, Mizutani M, Zucker CL, Lorenzi M. Expression of vascular endothelial growth factor in the human retina and in nonproliferative diabetic retinopathy. *Am J Pathol*. 1998;152:1453–1462.
31. Vinores SA, Youssri AI, Luna JD, et al. Upregulation of vascular endothelial growth factor in ischemic and non-ischemic human and experimental retinal disease. *Histol Histopathol*. 1997;12:99–109.
32. Engerman RL, Kern TS. Retinopathy in animal models of diabetes. *Diabetes Metab Rev*. 1995;11:109–120.
33. Hammes HP, Lin J, Bretzel RG, Brownlee M, Breier G. Upregulation of the vascular endothelial growth factor/vascular endothelial growth factor receptor system in experimental background diabetic retinopathy of the rat. *Diabetes*. 1998;47:401–406.

34. Joussen AM, Huang S, Poulaki V, et al. In vivo retinal gene expression in early diabetes. *Invest Ophthalmol Vis Sci*. 2001;42:3047–3057.
35. Simpson DA, Murphy GM, Bhaduri T, Gardiner TA, Archer DB, Stitt AW. Expression of the VEGF gene family during retinal vasoobliteration and hypoxia. *Biochem Biophys Res Commun*. 1999; 262:333–340.
36. Stitt AW, Simpson DA, Boocock C, Gardiner TA, Murphy GM, Archer DB. Expression of vascular endothelial growth factor (VEGF) and its receptors is regulated in eyes with intra-ocular tumours. *J Pathol*. 1998;186:306–312.
37. Agardh E, Bruun A, Agardh CD. Retinal glial cell immunoreactivity and neuronal cell changes in rats with STZ-induced diabetes. *Curr Eye Res*. 2001;23:276–284.
38. Winkler BS, Starnes CA, Sauer MW, Firouzgan Z, Chen SC. Cultured retinal neuronal cells and Muller cells both show net production of lactate. *Neurochem Int*. 2004;45:311–320.
39. Dalton SJ, Mitchell DC, Whiting CV, Tarlton JF. Abnormal extracellular matrix metabolism in chronically ischemic skin: a mechanism for dermal failure in leg ulcers. *J Invest Dermatol*. 2005;125: 373–379.
40. Norman JT, Orphanides C, Garcia P, Fine LG. Hypoxia-induced changes in extracellular matrix metabolism in renal cells. *Exp Nephrol*. 1999;7:463–469.
41. Chen YF, Feng JA, Li P, et al. Dominant negative mutation of the tgf-beta receptor blocks hypoxia-induced pulmonary vascular remodeling. *J Appl Physiol*. 2006;100:564–571.
42. Martin PM, Roon P, Van Ells TK, Ganapathy V, Smith SB. Death of retinal neurons in streptozotocin-induced diabetic mice. *Invest Ophthalmol Vis Sci*. 2004;45:3330–3336.
43. Park SH, Park JW, Park SJ, et al. Apoptotic death of photoreceptors in the streptozotocin-induced diabetic rat retina. *Diabetologia*. 2003;46:1260–1268.
44. Hancock HA, Kraft TW. Oscillatory potential analysis and ergs of normal and diabetic rats. *Invest Ophthalmol Vis Sci*. 2004;45: 1002–1008.
45. Fortune B, Schneck ME, Adams AJ. Multifocal electroretinogram delays reveal local retinal dysfunction in early diabetic retinopathy. *Invest Ophthalmol Vis Sci*. 1999;40:2638–2651.
46. Ewing FM, Deary IJ, Strachan MW, Frier BM. Seeing beyond retinopathy in diabetes: electrophysiological and psychophysical abnormalities and alterations in vision. *Endocr Rev*. 1998;19:462–476.
47. Jackson GR, Owsley C. Visual dysfunction, neurodegenerative diseases, and aging. *Neurol Clin*. 2003;21:709–728.
48. Li H, Telemaque S, Miller RE, Marsh JD. High glucose inhibits apoptosis induced by serum deprivation in vascular smooth muscle cells via upregulation of bcl-2 and bcl-xl. *Diabetes*. 2005;54: 540–545.
49. Levin LA, Schlamp CL, Spieldoch RL, Geszvain KM, Nickells RW. Identification of the bcl-2 family of genes in the rat retina. *Invest Ophthalmol Vis Sci*. 1997;38:2545–2553.
50. Tsang SH, Chen J, Kjeldbye H, et al. Retarding photoreceptor degeneration in pdegtm1/pdegtml mice by an apoptosis suppressor gene. *Invest Ophthalmol Vis Sci*. 1997;38:943–950.